Precision Pointing Control to and Accurate Target Estimation of a Non-Cooperative Vehicle

John Van Eepoel*, Julie Thienel† and Robert M. Sanner‡

In 2004, NASA began investigating a robotic servicing mission for the Hubble Space Telescope (HST). Such a mission would not only require estimates of the HST attitude and rates in order to achieve capture by the proposed Hubble Robotic Vehicle (HRV), but also precision control to achieve the desired rate and maintain the orientation to successfully dock with HST. To generalize the situation, HST is the target vehicle and HRV is the chaser. This work presents a nonlinear approach for estimating the body rates of a non-cooperative target vehicle, and coupling this estimation to a control scheme. Non-cooperative in this context relates to the target vehicle no longer having the ability to maintain attitude control or transmit attitude knowledge.

INTRODUCTION

The Hubble Space Telescope (HST) was launched in 1990 and has undergone four servicing missions throughout its mission lifetime to replace instruments, sensors, solar arrays, power units, and cooling systems. Additional servicing will again be necessary to extend HST's science life. The batteries are predicted to fail as early as 2009, and the pointing control system may be reduced to a two-gyro mode by as early as 2007. On March 12, 2004 former NASA Administrator Sean O'Keefe asked the HST program to investigate robotic servicing of the HST to extend the science life. The original robotic servicing mission concept, referred to here as the Hubble Robotic Vehicle (HRV), included two vehicles, a de-orbit module and an ejection module with a robotic arm for servicing. The HRV must be capable of docking with HST, regardless of the orientation or rotation rate of HST. In order for the HRV to dock with HST, the HRV must be capable of first estimating the attitude and rate of HST and then matching the HST attitude and rates.

This work applies an approach to estimate the attitude and rates of a non-cooperative target vehicle, and then uses the attitude and rate estimates as the desired state of the chaser vehicle. The target vehicle attitude estimate is provided by a vision or feature-based sensor. The target rate is determined with the nonlinear estimation approach presented in reference 1. The estimator is exponentially stable in the absence of any measurement errors, and remains robust to bounded perturbations resulting from uncertainties in the measured target attitude. The estimator then provides the desired rate for the nonlinear passivity-based control scheme presented in reference 2. The nonlinear controller is asymptotically stable in the absence of any disturbances. The actual attitude of the chaser vehicle is

*NASA Goddard Space Flight Center, Flight Dynamics Analysis Branch, Greenbelt, MD 20771, phone: 301-286-9216, fax: 301-286-0369, email: john.m.vaneepoel@nasa.gov

†NASA Goddard Space Flight Center, Flight Dynamics Analysis Branch, Greenbelt, MD 20771, phone: 301-286-9033, fax: 301-286-0369, email: julie.thienel@nasa.gov

‡University of Maryland, Department of Aerospace Engineering, College Park, Maryland, 20742 phone: 301-405-1928, fax: 301-314-9001, email: rmsanner@eng.umd.edu

assumed to be available from an accurate sensor such as a star tracker. The chaser vehicle rates are provided by gyros, assumed calibrated for alignment and scale factor errors. Reference 3 shows that the nonlinear control algorithm remains robust to gyro bias errors and bounded noise disturbances when coupled with a nonlinear gyro bias estimation scheme. The stability of the nonlinear control, given bounded estimates of the desired state of the chaser vehicle, is explored.

The next section gives an overview of the mathematical terms. Then the nonlinear estimation algorithm is summarized, followed by a summary of the nonlinear control algorithm. We then present the results of several scenarios, applied to HST-HRV. Finally conclusions are given along with future considerations.

ATTITUDE DEFINITIONS

The attitude of a spacecraft can be represented by a quaternion, consisting of a rotation angle and unit rotation vector $\boldsymbol{e}$, known as the Euler axis, and a rotation ϕ about this axis so that[4]

$$\boldsymbol{q} = \begin{bmatrix} e\sin(\frac{\phi}{2}) \\ \cos(\frac{\phi}{2}) \end{bmatrix} = \begin{bmatrix} \boldsymbol{\varepsilon} \\ \eta \end{bmatrix} \tag{1}$$

where $\boldsymbol{q}$ is the quaternion, partitioned into a vector part, $\boldsymbol{\varepsilon}$, and a scalar part, η. The target attitude quaternion is designated as $\boldsymbol{q}_t$, which defines the rotation from inertial to the target spacecraft body coordinates. The chase vehicle attitude quaternion is designated as $\boldsymbol{q}_c$.

The rotation, or attitude, matrix can be computed from the quaternion components as[4]

$$R = R(\boldsymbol{q}) = (\eta^2 - \boldsymbol{\varepsilon}^T\boldsymbol{\varepsilon})\mathrm{I}_3 + 2\boldsymbol{\varepsilon}\boldsymbol{\varepsilon}^T - 2\eta S(\boldsymbol{\varepsilon}) \tag{2}$$

where I_3 is a 3x3 identity matrix and $S(\boldsymbol{\varepsilon})$ is a matrix representation of the vector cross product operation.

$$S(\boldsymbol{\varepsilon}) = \begin{bmatrix} 0 & -\varepsilon_z & \varepsilon_y \\ \varepsilon_z & 0 & -\varepsilon_x \\ -\varepsilon_y & \varepsilon_x & 0 \end{bmatrix}$$

Note also that $R(\boldsymbol{q})\boldsymbol{\varepsilon} = \boldsymbol{\varepsilon}$. The derivative of $R(\boldsymbol{q})$ is given as[4]

$$\dot{R}(\boldsymbol{q}) = -S(\boldsymbol{\omega})R(\boldsymbol{q}) \tag{3}$$

where $\boldsymbol{\omega}$ is the angular velocity in body coordinates.

A relative rotation between coordinate frames is computed as[5]

$$\tilde{\boldsymbol{q}}_{rel} = \begin{bmatrix} \tilde{\boldsymbol{\varepsilon}} \\ \tilde{\eta} \end{bmatrix} = \boldsymbol{q}_1 \otimes \boldsymbol{q}_2^{-1} = \begin{bmatrix} \eta_2 I - S(\boldsymbol{\varepsilon}_2) & -\boldsymbol{\varepsilon}_2 \\ \boldsymbol{\varepsilon}_2^T & \eta_2 \end{bmatrix} \begin{bmatrix} \boldsymbol{\varepsilon}_1 \\ \eta_1 \end{bmatrix} \tag{4}$$

Using the definition given in equation 4, the relative attitude quaternion from the chase vehicle body coordinates to the target body coordinates is then

$$\tilde{\boldsymbol{q}}_{ct} = \boldsymbol{q}_t \otimes \boldsymbol{q}_c^{-1} \tag{5}$$

The angular velocity of the target vehicle body coordinates with respect to inertial space, resolved in target body coordinates, is designated as $\boldsymbol{\omega}_t$. Similarly the angular velocity of the chase vehicle in chase vehicle body coordinates is designated as $\boldsymbol{\omega}_c$.

TARGET VEHICLE NONLINEAR ESTIMATOR

The angular velocity estimator is intended for the scenario in which the target vehicle is non-cooperative. For example, in the HST robotic servicing mission the estimator would be used in the event that the HST batteries have died and no telemetry is available from HST. The chase vehicle is equipped with an accurate quaternion star tracker, which provides $\boldsymbol{q}_c$, and a sensor system which produces a measurement of the relative quaternion, $\tilde{\boldsymbol{q}}_{tc}$. The unknown target vehicle angular velocity is estimated in the inertial coordinate system through the estimation of the inertial angular momentum. The target vehicle angular velocity in body coordinates is computed by a transformation of the inertial angular velocity. The development and stability analysis of the algorithm are provided in reference 1. The algorithm is summarized here.

The system equations consist of the kinematic equation for the target vehicle attitude quaternion and Euler's equation for the target vehicle given in inertial coordinates

$$\dot{\boldsymbol{q}}_t = \frac{1}{2}Q(\boldsymbol{q}_t)\boldsymbol{\omega}_t = \frac{1}{2}Q(\boldsymbol{q}_t)R_t\boldsymbol{\omega}_{i,t} = \frac{1}{2}Q(\boldsymbol{q}_t)I_t^{-1}R_t\boldsymbol{h}_{i,t} \tag{6}$$

$$\dot{\boldsymbol{h}}_{i,t} = T_{i,t} \tag{7}$$

where I_t is the target vehicle inertia matrix in body coordinates, assumed to be constant. Note that $I_{i,t} = R_t^T I_t R_t$, where $I_{i,t}$ is the inertia matrix in inertial coordinates and R_t is the target vehicle attitude matrix defining the transformation from inertial to target body coordinates. $T_{i,t}$ is the external torque acting on the target vehicle, resolved in inertial coordinates, and

$$Q(\boldsymbol{q}_t) = \begin{bmatrix} \eta_t \mathrm{I}_3 + S(\boldsymbol{\varepsilon}_t) \\ -\boldsymbol{\varepsilon}_t^T \end{bmatrix} = \begin{bmatrix} Q_1(\boldsymbol{q}_t) \\ -\boldsymbol{\varepsilon}_t^T \end{bmatrix} \tag{8}$$

where, by inspection, $Q_1(\boldsymbol{q}_t) = \eta_t \mathrm{I}_3 + S(\boldsymbol{\varepsilon}_t)$.

The predicted target vehicle quaternion as defined as

$$\hat{\boldsymbol{q}}_t = \begin{bmatrix} \hat{\boldsymbol{\varepsilon}}_t \\ \hat{\eta}_t \end{bmatrix}$$

The attitude error is defined as the relative orientation between the predicted attitude $\hat{\boldsymbol{q}}_t$ and the measured attitude, $\boldsymbol{q}_t$, computed from equation 4 from the measured relative attitude quaternion and the measured chase vehicle attitude quaternion. The estimator attitude error is

$$\tilde{\boldsymbol{q}}_t = \begin{bmatrix} \tilde{\boldsymbol{\varepsilon}}_t \\ \tilde{\eta}_t \end{bmatrix} = \boldsymbol{q}_t \otimes \hat{\boldsymbol{q}}_t^{-1} \tag{9}$$

The state estimators for the HST attitude and angular momentum are defined as

$$\dot{\hat{\boldsymbol{q}}}_t = \frac{1}{2}Q(\hat{\boldsymbol{q}}_t)R(\tilde{\boldsymbol{q}}_t)^T[I_t^{-1}R_t\hat{\boldsymbol{h}}_{i,t} + k\tilde{\boldsymbol{\varepsilon}}_t \mathrm{sign}(\tilde{\eta}_t)] \tag{10}$$

$$\dot{\hat{\boldsymbol{h}}}_{i,t} = T_{i,t} + \frac{\beta}{2}R_t^T I_t^{-1}\tilde{\boldsymbol{\varepsilon}}_t \mathrm{sign}(\tilde{\eta}_t) \tag{11}$$

The term $R(\tilde{\boldsymbol{q}}_t)^T$ in equation 10 transforms the angular velocity terms from the body frame to the predicted attitude frame. The gain k is chosen as a positive constant. Similarly, the learning rate, β, is also a positive constant. Essentially, $\hat{\boldsymbol{q}}_t$ is a prediction of the attitude at time t, propagated with the kinematic equation using the estimated angular momentum.

The error equations are given as

$$\dot{\tilde{\boldsymbol{q}}}_t = \frac{1}{2}Q(\tilde{\boldsymbol{q}}_t)(I_t^{-1}R_t\boldsymbol{h}_{i,t} - I_t^{-1}R_t\hat{\boldsymbol{h}}_{i,t} - k\tilde{\boldsymbol{\varepsilon}}_t \mathrm{sign}(\tilde{\eta}_t)) \tag{12}$$

Let $\tilde{\boldsymbol{h}}_{i,t} = \boldsymbol{h}_{i,t} - \hat{\boldsymbol{h}}_{i,t}$. The derivative of $\tilde{\boldsymbol{h}}_{i,t}$ is

$$\dot{\tilde{\boldsymbol{h}}}_{i,t} = -\frac{\beta}{2} R_t^T I_t^{-1} \tilde{\boldsymbol{\varepsilon}}_t \text{sign}(\tilde{\eta}_t) \tag{13}$$

Note that the equilibrium states for 12 and 13 are

$$\begin{bmatrix} \tilde{\boldsymbol{q}}_t^T & \tilde{\boldsymbol{h}}_{i,t}^T \end{bmatrix} = \begin{bmatrix} 0 & 0 & 0 & \pm 1 & 0 & 0 & 0 \end{bmatrix}$$

In the absence of any errors, equations 12 and 13 are exponentially stable, i.e $\hat{\boldsymbol{\omega}}_t \rightarrow \boldsymbol{\omega}_t$ exponentially fast.[1]

Reference 1 examines the stability of the nonlinear estimator given errors in the relative attitude quaternion. The measurement of the relative attitude quaternion from the vision and feature based sensor was the largest source of error for HRV. When the true quaternion is unknown, equations 10 and 11 cannot be implemented. Instead, the erroneous measured attitude $\boldsymbol{q}_{t,m}$ is used in place of $\boldsymbol{q}_t$, resulting in

$$\dot{\hat{\boldsymbol{q}}}_t = \frac{1}{2} Q(\hat{\boldsymbol{q}}_t) R(\tilde{\boldsymbol{q}}_{t,m})^T [I_v^{-1} R_{t,m} \hat{\boldsymbol{h}}_{i,t} + k \tilde{\boldsymbol{\varepsilon}}_{t,m} \text{sign}(\tilde{\eta}_{t,m})] \tag{14}$$

$$\dot{\hat{\boldsymbol{h}}}_{i,t} = \hat{T}_{i,t} + \frac{\beta}{2} R_{t,m}^T I_t^{-1} \tilde{\boldsymbol{\varepsilon}}_{t,m} \text{sign}(\tilde{\eta}_{t,m}) \tag{15}$$

$\hat{T}_{i,t}$ is the estimated external torque. The estimator, however, remains robust to disturbances in the relative attitude measurement. The addition of a leakage term ensures that the system remains bounded in the event of unusually large disturbances.[1]

CHASE VEHICLE CONTROL ALGORITHM

Prior to docking with the target vehicle, the chase vehicle control system must force the chase vehicle to match the attitude and attitude rates of the target vehicle to within some mission specific tolerance. In the non-cooperative scenario considered here, the target vehicle attitude and rates are provided by the nonlinear estimator of the previous section. The chase vehicle is equipped with star trackers and calibrated gyros to provide the necessary feedback signals to the control algorithm. In this work we consider the nonlinear adaptive controller of reference 2.

The attitude dynamics of the chase vehicle, modelled as a rigid spacecraft, are given as (the time dependence is omitted for clarity)

$$I_c \dot{\boldsymbol{\omega}}_c - S(I_c \boldsymbol{\omega}_c + \boldsymbol{h}_c)\boldsymbol{\omega}_c = \boldsymbol{u} + \dot{\boldsymbol{h}}_c$$

where I_c is the inertia matrix, $\boldsymbol{u}$ is the applied external torque, $\boldsymbol{\omega}_c$ is the angular velocity, and $\boldsymbol{h}_c$ is the wheel momentum in body coordinates. The goal of the control law is to force the attitude of the chase vehicle, $\boldsymbol{q}_c$ to asymptotically track the target vehicle attitude, $\boldsymbol{q}_t$, and the target vehicle rate, $\boldsymbol{\omega}_t$. The attitude tracking error is computed with equation 4 as

$$\tilde{\boldsymbol{q}}_{tc} = \begin{bmatrix} \tilde{\boldsymbol{\varepsilon}}_{tc} \\ \tilde{\eta}_{tc} \end{bmatrix} = \boldsymbol{q}_c \otimes \boldsymbol{q}_t^{-1}$$

The rate tracking error is given as

$$\tilde{\boldsymbol{\omega}}_{tc} = \boldsymbol{\omega}_c - R(\tilde{\boldsymbol{q}}_{tc})\boldsymbol{\omega}_t$$

where $R(\tilde{\boldsymbol{q}}_{tc})$ transforms the angular velocity from the target vehicle body frame to the chase vehicle body frame.

The control law is given as

$$\boldsymbol{u} + \dot{\boldsymbol{h}}_c = -K_D \boldsymbol{s}(t) + I_c \boldsymbol{\alpha}_r - S(I_c \boldsymbol{\omega}_c + \boldsymbol{h}_c)\boldsymbol{\omega}_r$$

K_D is any symmetric, positive definite matrix and $\boldsymbol{s}$ is an error defined as

$$\boldsymbol{s} = \tilde{\boldsymbol{\omega}}_{tc} + \lambda \tilde{\boldsymbol{\varepsilon}}_{tc} = \boldsymbol{\omega}_c - \boldsymbol{\omega}_r$$

where λ is any positive constant. The reference angular velocity $\boldsymbol{\omega}_r$ is computed as

$$\boldsymbol{\omega}_r = R(\tilde{\boldsymbol{q}}_{tc})\boldsymbol{\omega}_t - \lambda \tilde{\boldsymbol{\varepsilon}}_{tc}$$

The derivative of $\boldsymbol{\omega}_r$ is given as

$$\boldsymbol{\alpha}_r = \dot{\boldsymbol{\omega}}_r = R(\tilde{\boldsymbol{q}}_{tc})\dot{\boldsymbol{\omega}}_t - S(\tilde{\boldsymbol{\omega}}_{tc})R(\tilde{\boldsymbol{q}}_{tc})\boldsymbol{\omega}_t - \lambda Q_1(\tilde{\boldsymbol{q}}_{tc})\tilde{\boldsymbol{\omega}}_{tc}$$

Asymptotically perfect tracking is obtained with the above control scheme, given noise free measurements of the states $\boldsymbol{\omega}_c$ and $\boldsymbol{q}_c$. Reference 3 also shows that the control scheme is robust to gyro bias errors and bounded noise disturbances. (The gyros are assumed to be calibrated for scale factor and misalignment errors prior to the approach and capture phase. Gyro bias errors can be estimated a priori as well.)

In a typical control application the desired states are well defined. In this work, however, the desired states are estimated with the nonlinear estimator outlined in the previous section. The nonlinear estimator provides continuous estimates of the desired attitude, desired rate, and derivative of the desired rate. The desired attitude is provided by the estimator as $\hat{\boldsymbol{q}}_t$. The control error is then computed as

$$\tilde{\boldsymbol{q}}_{tc} = \begin{bmatrix} \tilde{\boldsymbol{\varepsilon}}_{tc} \\ \tilde{\eta}_{tc} \end{bmatrix} = \boldsymbol{q}_c \otimes \hat{\boldsymbol{q}}_t^{-1}$$

The desired rate, $\boldsymbol{\omega}_t$ in the target body coordinates, is computed from the estimated angular momentum as

$$\boldsymbol{\omega}_t = I_t^{-1} R(\hat{\boldsymbol{q}}_t)\hat{\boldsymbol{h}}_{i,t}$$

The chase vehicle desired angular acceleration is then

$$\dot{\boldsymbol{\omega}}_t = I_t^{-1}[\dot{R}(\hat{\boldsymbol{q}}_t)\hat{\boldsymbol{h}}_{i,t} + R(\hat{\boldsymbol{q}}_t)\dot{\hat{\boldsymbol{h}}}_{i,t}]$$

Substituting for $\dot{R}(\hat{\boldsymbol{q}}_t)$ from equation 3 and $\dot{\hat{\boldsymbol{h}}}_{i,t}$ from equation 15, $\dot{\boldsymbol{\omega}}_t$ is written as

$$\dot{\boldsymbol{\omega}}_t = I_t^{-1}[S(\hat{\boldsymbol{\omega}}_t)R(\hat{\boldsymbol{q}}_t)\hat{\boldsymbol{h}}_{i,t} + R(\hat{\boldsymbol{q}}_t)(\hat{T}_{i,t} + \frac{\beta}{2} R_{t,m}^T I_t^{-1} \tilde{\boldsymbol{\varepsilon}}_{t,m} \mathrm{sign}(\tilde{\eta}_{t,m}))]$$

where $\tilde{\boldsymbol{\varepsilon}}_{t,m}$, $\tilde{\eta}_{t,m}$, and $R_{t,m}$ are all calculated using the measured attitude. The control algorithm will asymptotically track the estimated states. Since the estimator provides a bounded estimate of the true states in the presence of measurement errors, the chase vehicle will track the target vehicle states within the bounds of the estimator.

SIMULATION RESULTS

The algorithms outlined in the previous sections are tested in two simulation environments. Both simulations are based on an HRV-HST rendezvous scenario. The first simulation is developed in Matlab. The Matlab simulation gives a high level indication of the performance of the combined estimator and control algorithm. Then the simulation is developed in the NASA Goddard Space Flight Center simulation environment known as Freespace (FSP). FSP is a C-based high fidelity, modular

simulation environment containing gravity and aerodynamic torque models, multi-body dynamics and control for n-spacecraft. FSP utilizes shared memory with a modular structure to enable simultaneous algorithm processing and graphical visualization. The results from the Matlab simulation are presented first, followed by results from FSP.

The HST (target) inertia is[6]

$$I_t = \begin{bmatrix} 36046 & -706 & 1491 \\ -706 & 86868 & 449 \\ 1491 & 449 & 93848 \end{bmatrix} kg \cdot m^2$$

The HRV (chase) inertia matrix is[6]

$$I_c = \begin{bmatrix} 18748 & 525 & -2197 \\ 525 & 55903 & 1366 \\ -2197 & 1366 & 53025 \end{bmatrix} kg \cdot m^2$$

Both algorithms are initially tested without any errors. In both cases, the initial attitude quaternions are identity, $\boldsymbol{q}_t = \hat{\boldsymbol{q}}_t = [0, 0, 0, 1]$. The initial HST angular velocity estimate is zero, $\hat{\boldsymbol{\omega}}_t = [0, 0, 0]$, and the true initial angular velocity is $\boldsymbol{\omega}_t = [-0.04, -0.01, 0.14]$ deg/sec.

Figures 1 and 2 show the attitude control error and the angular velocity control error with perfect measurements. The estimator runs for 5000 seconds before the control algorithm is started. The final attitude control error and rate control error (magnitude) are 0.01 deg and $1.6e{-}5$ deg/sec, respectively, and both are still converging.

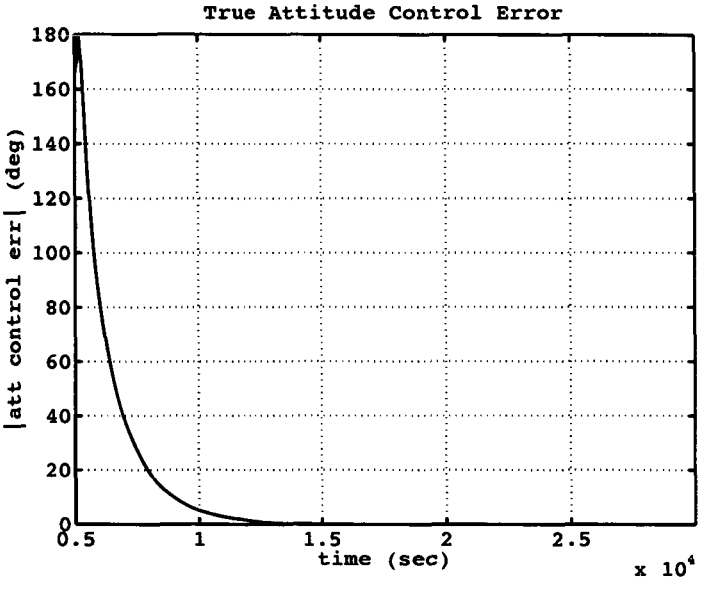

Figure 1 True Attitude Control Errors, No Measurement Errors

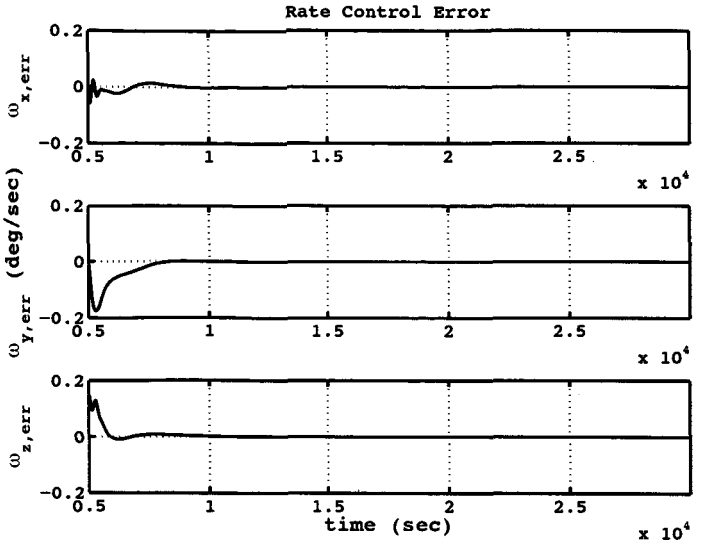

Figure 2 True Angular Velocity Control Errors, No Measurement Errors

Next, the measured attitude is chosen randomly with a 10 degree uncertainty. The estimator is initialized with the first attitude measurement. The HRV attitude is initialized at $\boldsymbol{q}_c = [0, 1, 0, 0]$. The initial HRV angular velocity is $\boldsymbol{\omega}_c = [0, 0, 0]$ deg/sec. Figures 3 and 4 are samples of the attitude control error and the angular velocity control error. Here the final attitude control error is approximately 1 deg and the final rate control error is 0.001 deg/sec, both are within the long range requirements for the HRV capture. Reducing the attitude error to 1 degree results in final attitude and rate errors of 0.04 deg and 0.00017 deg/sec, respectively, which meet the close range requirements. (The measured attitude error is expected to improve as the approach distance decreases.)

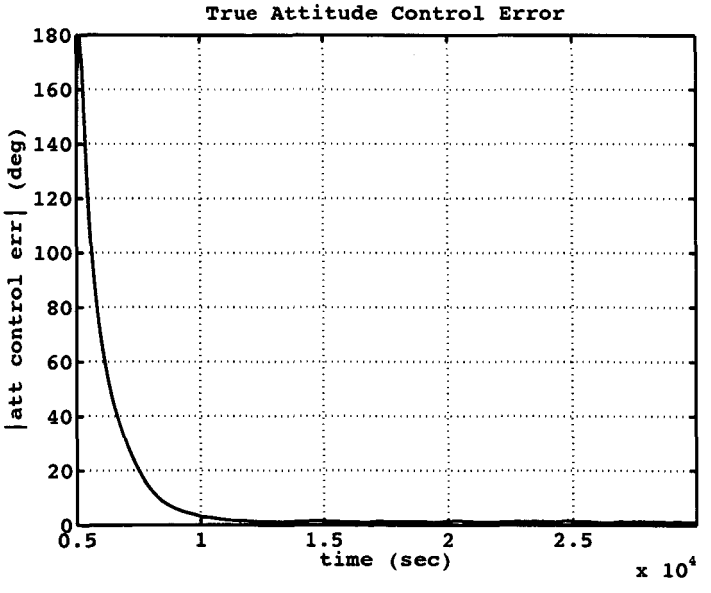

Figure 3 True Attitude Control Errors, 10 Degree Attitude Measurement Errors

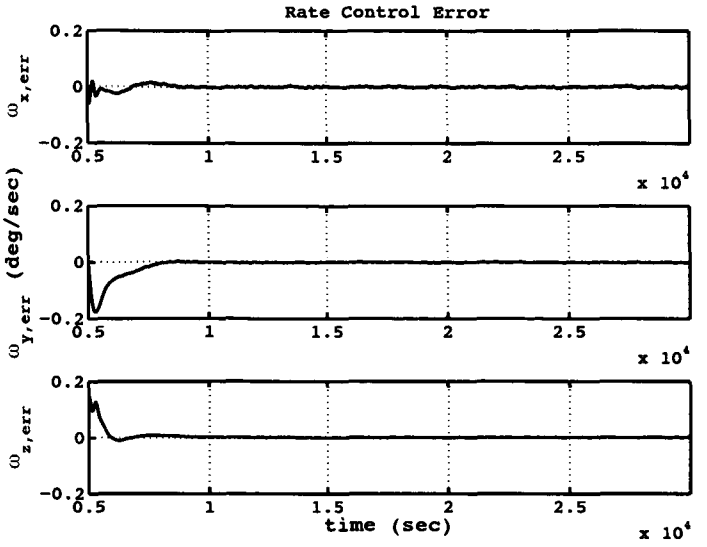

Figure 4 True Angular Velocity Control Errors, 10 Degree Attitude Measurement Errors

The simulation was then repeated 100 times, each with a different random measured attitude sample, again with an uncertainty of 10 degrees. Figure 5 shows the true attitude control error for 100 different test cases. In all cases the controller is converging. The final average attitude error for all 100 cases is 1.3 deg. Figure 6 shows the true angular rate error. Again, the controller is converging. The average angular velocity control errors at the end of the tests are

$$\tilde{\omega}_{tc}(avg \;\; in \;\; deg/sec) = \begin{bmatrix} -0.00032 \\ 0.00021 \\ -0.00036 \end{bmatrix}$$

Next, the algorithms are tested in the FSP high fidelity simulator. The Freespace truth model contains gravity gradient and aerodynamic external torques acting on HRV, and gravity gradient only on HST. The HRV gravity gradient torques are input to the control algorithm as a feed forward torque, leaving the aerodynamic torque as a disturbance to the controller. The scenario developed for these results places the HRV at the 50 m hold point on the HST -V1 axis (boresight axis), which is the point at which the rescue mission would have begun to match the attitude and angular rate of HST for docking. The initial angular rate of HST is the same as that assumed for the Matlab simulation.

The estimator performance in FSP compares to the results in reference 1, though with a longer convergence time. The attitude of HRV is initially controlled using a coarse attitude control with no roll constraint, until 15000 sec (4 h 10 min) when the target attitude tracking controller is enabled. Figures 7 and 8 show the magnitude of the true attitude control error and the true angular rate error. The magnitudes of the attitude control error converge to 0.02 deg at the end but vary as high as 0.15 deg. The rate error does not have as much variation and converges to $2.8e{-}5$ deg/sec.

Then, sensor noise is added to the relative quaternion measurement by corrupting the true relative attitude measurement with a randomly generated quaternion with a 3σ magnitude of 10 deg, as in the Matlab simulation. Figure 9 shows the magnitude of the true attitude controller error, which converges to 0.75 deg, with only slight variations above 1 deg. Figure 10 shows the convergence of the true angular rate error, which converges to 0.00091 deg/sec. For a relative quaternion measurement with only 1 deg of error, the controller attitude and rate errors converge to 0.075 deg and 0.0024 deg/sec, respectively.

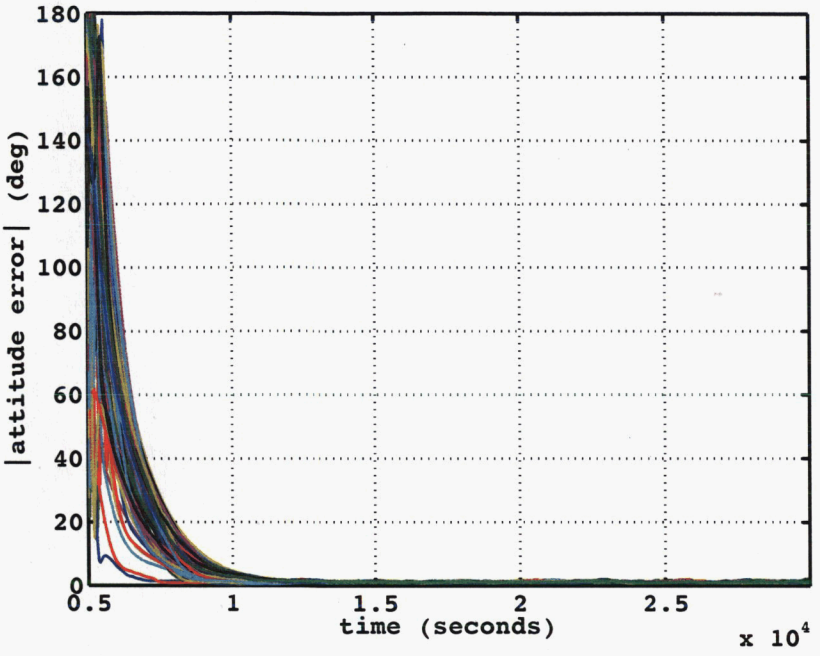

Figure 5 True Attitude Control Errors, 100 Test Cases with Random Attitude Measurement Errors

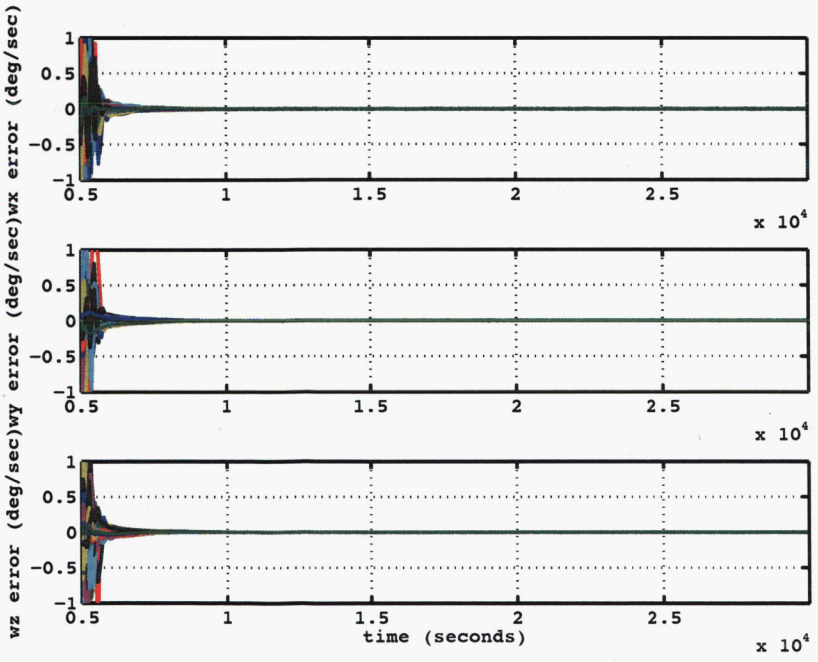

Figure 6 True Angular Velocity Control Errors, 100 Tests Cases with Random Attitude Measurement Errors

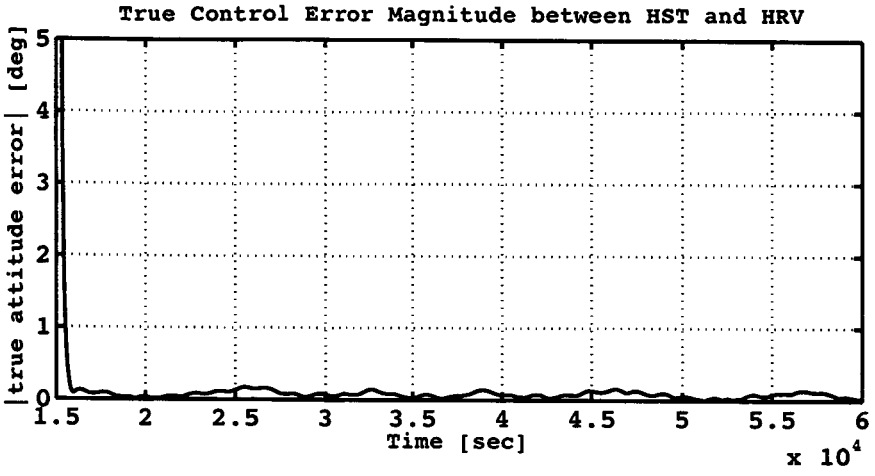

Figure 7 True Attitude Control Errors from Freespace, No Measurement Errors

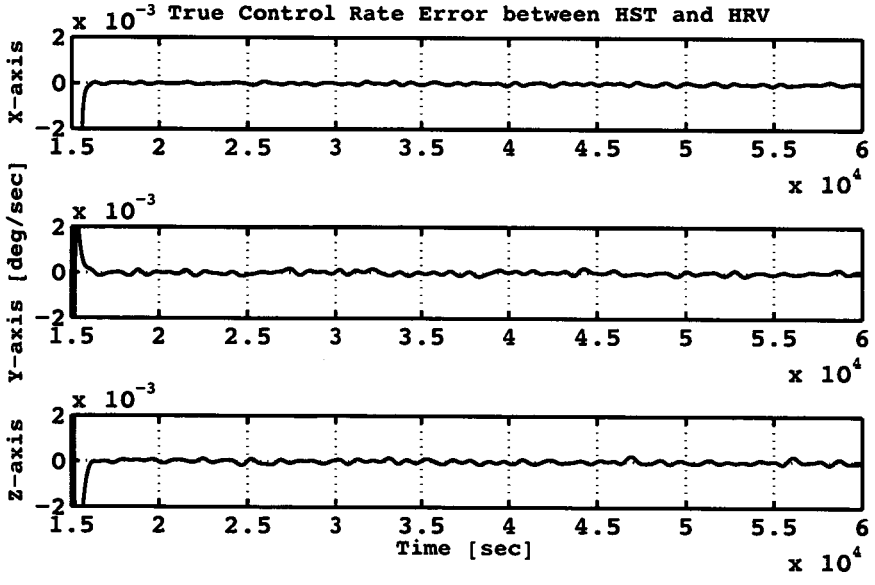

Figure 8 True Rate Control Errors from Freespace, No Measurement Errors

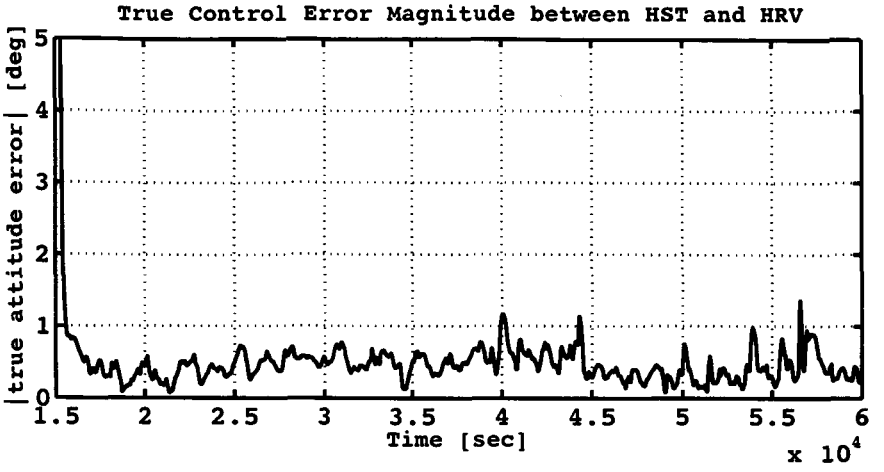

Figure 9 True Attitude Control Errors from Freespace, 10 deg Measurement Error

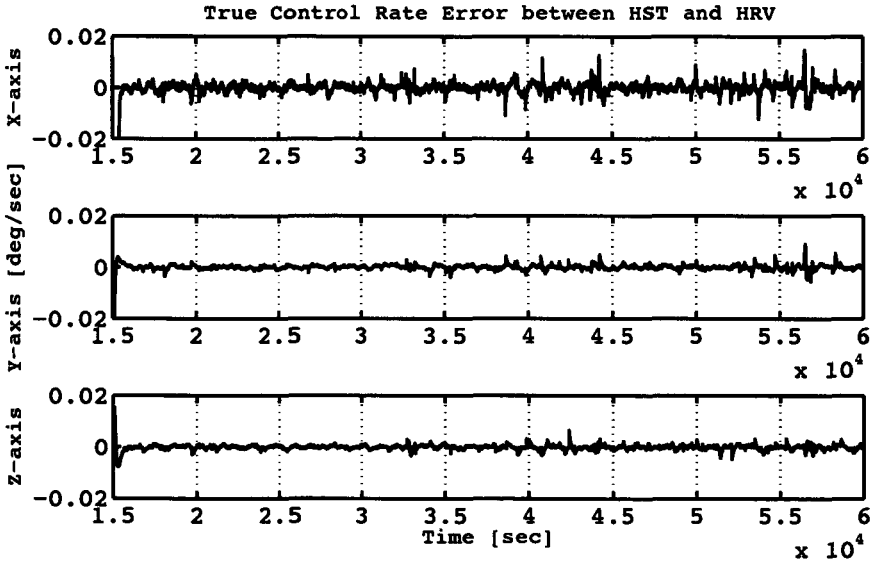

Figure 10 True Rate Control Errors from Freespace, 10 deg Measurement Error

These results confirm the findings of the low fidelity Matlab simulation, and also enable further experiments to characterize the estimator / controller interaction and behavior under various conditions (i.e. varying the measurement error, the initial target rates, and dynamic model fidelity).

CONCLUSIONS

An approach for estimating the attitude and rates of a non-cooperative target vehicle and then controlling the chase vehicle to match the estimated attitude and rates is presented. The attitude and rates are estimated with a nonlinear estimation algorithm that is robust to measured attitude errors. The nonlinear control algorithm is asymptotically stable in the absence of errors, and remains robust given gyro measurement errors. The algorithms are applied to the HST robotic servicing mission and are tested first with a Matlab simulation, introducing a random attitude measurement error of 10 degrees. A Monte Carlo simulation demonstrates that the combined algorithms are stable and converge to less than 1.3 deg and 0.00052 deg/sec in attitude and rate control errors (magnitude), respectively. The algorithms are then tested in a high performance simulation environment known as Freespace. Again, the combined algorithms are stable and converge to final error less than 0.075 deg and 0.0024 deg/sec with a measurement error of 1 deg.

Future work will expand the simulation scenario in Freespace. The vision sensors will be modelled and used to provide the relative attitude measurement. Additional fidelity will be added to the wheel models and the chase vehicle gyros, along with a star tracker based attitude estimation algorithm for the chase vehicle.

ACKNOWLEDGEMENT

The authors would like to acknowledge the tireless work of Steve Queen in providing the Freespace simulation environment to test this algorithm, along with offering his counsel in analyzing the results.

REFERENCES

1. Thienel, J. K., Queen, S. Z., VanEepoel, J. M., and Sanner, R. M., "Hubble Space Telescope Angular Velocity Estimation During the Robotic Servicing Mission," *AIAA Guidance, Navigation, and Control Conference*, No. 2005-6396, San Francisco, California, August 2005.

2. Egeland, O. and Godhavn, J., "Passivity-Based Adaptive Attitude Control of a Rigid Spacecraft," *IEEE Transactions on Automatic Control*, Vol. 39, No. 4, April 1994, pp. 842–846.

3. Thienel, J., *Nonlinear Observer/Controller Designs for Spacecraft Attitude Control Systems with Uncalibrated Gyros*, Ph.D. thesis, University of Maryland, 2004.

4. Shuster, M. D., "A Survey of Attitude Representations," *The Journal of Astronautical Sciences*, Vol. 41, No. 4, October-December 1993, pp. 439–517.

5. Sanner, R. M., "Adaptive Attitude Control Using Fixed and Dynamically Structured Neural Networks," *AIAA Guidance, Navigation, and Control Conference*, No. 96-3891, San Diego, California, July 1996.

6. Queen, S., "HRV GNC Peer Review, Flight Performance Analysis," Tech. rep., NASA Goddard Space Flight Center, 2004.